UDC 519.2: 621.313.13
Original scientific paper
Received: 15.09.2000.

Determination of variation of slot permeance in induction machines including slot bridge saturation

Hanifi Guldemir
University of Firat, Technical Education Faculty, Department of Electronics & Computer Science, Elazığ, Turkey
e-mail: hguldemir@firat.edu.tr

SUMMARY

The paper uses finite element analysis for obtaining permeance variation around the airgap and its harmonic content for a squirrel-cage closed-slot induction motor. The paper also presents a similar solution for the variation in slot permeance which takes into account the core saturation due to the nonlinear characteristics of the magnetic material and the saturation due to induced rotor bar currents which are of great interest, which has not been available so far. The permeance variation is derived from the stored energy which is obtained using the finite element (FE) field solution. The permeance distribution is then decomposed into the harmonic content by using Fast Fourier Transform. The dependence of the harmonic components on the rotor current is also given.

***Key words**: slot, airgap, permeance, induction motor, slot bridge saturation.*

1. INTRODUCTION

The nonuniform airgap due to the slots around the airgap produces permeance waves for the airgap which induces a series of harmonics in the airgap field known as slot permeance harmonics. These slot harmonics provides information for the determination of speed in sensorless speed prediction techniques [1], in the calculation of radial force, vibration and noise [2], in the calculation of surface losses [3], in the diagnosis, condition monitoring and fault detection in squirrel-cage induction motors [4, 5].

The techniques for calculating the permeance waves when the stator and rotor are slotted are conformal transformation [6] and formal Fourier series expansion [7]. Using these techniques restrictive assumptions are employed such as the slots are open and the magnetic material is unsaturated. Neither of these assumptions is appropriate for the rotor slots employed in modern induction motors. It is for this reason that these approaches are not used in the work presented in this study.

Open slots are not desirable as they introduce large permeance pulsation and this increases the effective airgap length. In machines with closed slots, infinite permeability of the iron can no longer be assumed since the slot bridges become saturated. The saturation of the slot bridges is a function of the approximate sinusoidally spatially distributed rotor currents [8]. Therefore slot bridge saturation is taken into account at the appropriate load condition.

2. FINITE ELEMENT ANALYSIS

The finite element method is based on the minimisation of Poisson's equation expressed in the functional form. The potentials at the nodes are described by describing functions. By substituting these functions into the functional equation, a set of simultaneous equations is obtained covering all nodes where potentials are not defined. The use of this technique allows the modelling of magnetic nonlinearities in the machine iron and the inclusion of induced currents in the rotor bar [9]. The FE method is well adapted to finding the flux distribution in an induction motor allowing for iron saturation and there are many papers dealing with its application and refinement. However, it can be computationally demanding for difficult geometries and those which change with time.

The most accurate way to calculate the magnetic field of the induction motor is to use the FE method. However, if large numbers of elements are used, this results in a large number of equations and long solution time, which requires a high performance mainframe computer or workstation. The problem is that if the influence of changes on a particular design feature of a

motor is to be investigated this requires repeated solutions. This extends the time required to formulate an understanding of the link between the design change and the effect it has upon the performance. In effect, the FE model produces accurate results but resembles experimental work to some degrees in that analytical equations can not be written to link cause and effect without a curve fitting the equations to the results obtained from a number of test runs.

The work presented in this study is aimed at increasing the understanding of the features of motor design which influence the magnitude of the slot permeance harmonics [10]. In other words, FE is used to examine the slot permeance and saturation effects in slot bridges and tooth tips where a fine description of the field distribution in the airgap of an induction motor is required.

Nowadays, commercial FE packages are widely used which reduces considerably the time needed to develop suitable machine models. MagNet was used for the work presented in this study.

2.1 Methodology of FE Analysis

FE approach for electric machines has been formulated in many papers [11-14]. A good review of the present state of art was given by Nakata et al. [15]. The area to be modelled is subdivided into an array of elements, normally triangles to allow flexibility in modelling complex shapes, with a node at each corner to form a mesh over which the magnetic vector potential $\boldsymbol{A}$ will be solved. Most solutions are still 2D and hence A acts in the z direction and behaves more like a scalar potential. The coarseness of the mesh may vary across the problem, being the finest where the field values will change rapidly with spatial position and coarser where the field is more constant. Thus, for example, the magnetic field in the tooth tips and the airgap of an induction motor will be in a high mesh density region. Conversely, the core backs will be in a low mesh density region. The magnetic potential across each element is generally modelled either by a linear or first order shape function. Higher order variations are used in some cases. A linear shape function means that the flux density, and hence the relative permeability, m_r, is constant in the element. The resulting elemental field equations can be assembled into a matrix equation normally by the connection matrix type approach forcing the common nodes on neighbouring elements to be at the same potential. The matrix equation contains an excitation vector related to the source currents and this is also obtained by transformation. A set of nodal field equations is thereby formed, one equation per node, relating the value of the magnetic vector potential, $\boldsymbol{A}_j$, at each node both to the values at adjacent nodes, to the boundary conditions specified for the problem and to the excitation currents:

$$[\boldsymbol{J}] = [\boldsymbol{S}][\boldsymbol{A}] \qquad (1)$$

where $[\boldsymbol{A}]$ is the column vector of the unknown nodal potentials and $[\boldsymbol{J}]$ is the excitation column vector.

Once the problem has been defined and once the excitation vector, $[\boldsymbol{J}]$, and the stiffness matrix, $[\boldsymbol{S}]$, have been initialised, the matrix equation is solved to find the nodal magnetic potentials. If saturation is to be included in the model, the flux densities in the motor (described in the model by the curl of the magnetic vector potential $[\boldsymbol{A}]$) depend on the magnetic properties of the magnetic steel. These however, depend on the flux densities in the motor. The model is therefore non-linear and the non-linearity of the materials is included by iterative modifications to the stiffness matrix, $[\boldsymbol{S}]$.

Once the nodal magnetic vector potentials are known, these are converted into more useful quantities such as flux density, saturation levels, induced voltages and torques by a post processor program. In a two dimensional analysis, the magnetic vector potential has only one component acting axially along the machine and the flux is restricted to the plane of the solution. The flux flowing between any two nodes in the mesh is obtained from the difference in the potential of nodes and their distance. The flux density can therefore be determined in each element in the cross-section of the motor and areas with excessive saturation can be identified. The spatial harmonics of the flux density distribution can also be determined.

2.2 Determination of slot permeance harmonics

The stator and rotor windings in induction motors are housed in slots on both sides of the airgap which then becomes nonuniform along the periphery. The presence of slotting in the magnetic core of an electrical machine causes a reduction of the airgap flux density over the slot opening. As a result of the variation of the permeance of the airgap, the actual airgap field pattern is not pure sinusoidal but has a cyclically varying field superimposed. Consequently, these variations produce permeance harmonics. The presence of the slots on the surface of the rotor and stator increase the effective airgap length and decrease the airgap permeance by restricting the airgap field to a degree depending on the airgap length, slot opening and slot width. Figure 1 shows the variation of the airgap flux density due to the slotting of one side of the airgap.

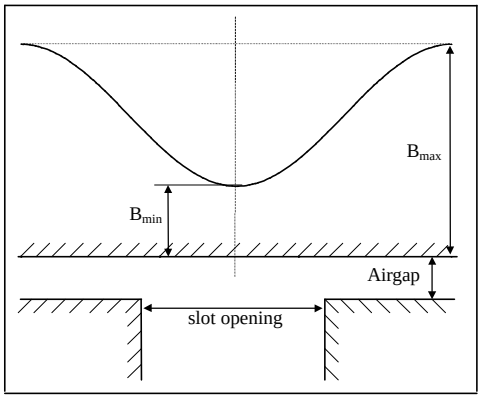

Fig. 1 Variation of airgap flux density over slot openings

2.3 Finite element model of the slots

The model set up is of the slot and adjacent proportion of the airgap which is solved by the FE package, MagNet. Only the slot bridge is assumed to saturate. The rest of the tooth is regarded as infinitely permeable. This can be seen in Figure 2 which shows the flux density of a complete slot model at a peak rotor current for full load where only slot bridge region shows significant saturation.

A Fortran programme is then used to determine the spatial permeance distribution from the stored energy since this is not available in the MagNet program. The permeance distribution is then decomposed into harmonic series.

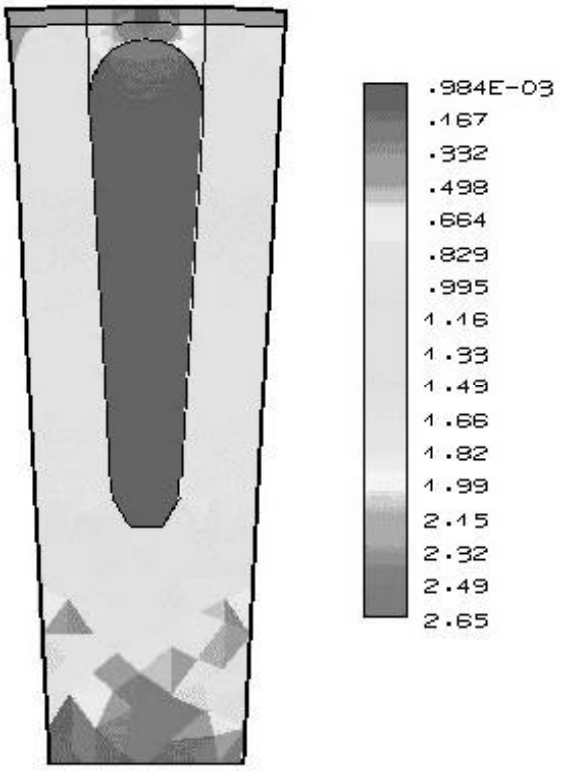

Fig. 2 Flux density in the complete slot pitch

3. SOLUTION OF THE FIELD PROBLEM

Figure 3 shows the finite element model of the slot, slot bridge and its mesh. The analytical procedure is divided into two steps. In the first step, in order to allow magnetic saturation, a nonlinear static magnetic field analysis is carried out with the actual current flowing through the bar.

The reluctivities which vary with the flux density in accordance with the saturation characteristics of the magnetic steel are obtained from the solution of the field in the parts of the magnetic circuit which are modelled as nonlinear. These are then saved in a data file. In the second step a linear finite element calculation is carried out using the saved reluctivities and the finite element model was excited by fixing the magnetic vector potentials at the extreme edges of the

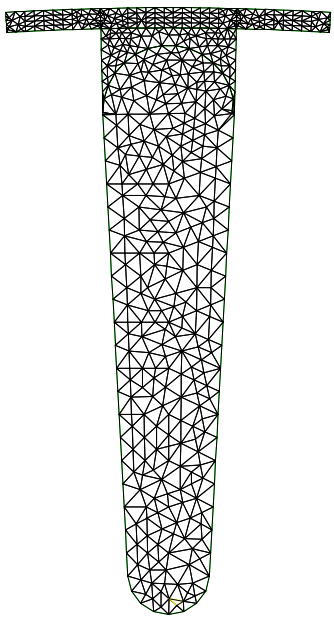

Fig. 3 Finite element model and mesh of a closed slot

problem. Since these edges occur midway across a tooth face it can be assumed that the flux in this region crosses the airgap radially so these edges can be treated as flux lines. Since the reluctivity of each element in the model is known, the permeance of the airgap is independent of the flux level so that the problem can be solved at an arbitrary flux level [16]. This is done by fixing the edges of the problem at different vector potentials which forces a known amount of flux across the airgap. An arbitrary flux level is satisfactory since the quantity which is being derived is the normalised permeance.

4. DETERMINATION OF THE NORMALISED AIRGAP PERMEANCES

The post-processor has been written to be as general as possible. It prompts the user to supply the information about the solution file such as: whether the rotor or stator slot has been solved, the filename where the solution is stored and the machine parameters. The post-processor then reads in the model information from the solution file skipping over those file sections which contain irrelevant information.

For the problem under consideration, the nodes which lie on the smooth iron surface and those lying on the slotted iron surface are identified. This enables the programme to output a plot of flux density along either of these two surfaces. The next stage is the calculation of permeances. The flux density is calculated from the value of the magnetic vector potential at each node as:

$$B_i = \frac{f_i}{D_i} = \frac{\boldsymbol{A}_i - \boldsymbol{A}_{i-1}}{x_i - x_{i-1}} \qquad (2)$$

Using the area of each element and the square of the flux density in each element, the stored magnetic energy can be obtained as:

$$Wm = \tfrac{1}{2} L \sum_e \frac{B_e^{\,2}}{m_e} D_e \qquad (3)$$

where B is the flux density of the element, L is the length and D_e is the area of the element. The sum is taken over all those elements in the region defining the permeance. The stored energy can also be defined from the flux flowing through the airgap permeances as:

$$Wm = \frac{1}{2}\frac{f^2}{L} \qquad (4)$$

Equating these two equations gives:

$$L = 2 * \frac{Wm}{f^2} \qquad (5)$$

where f is the flux density crossing the airgap in the area defined as the permeance. The permeances are assumed to be bounded by flux lines so that no flux enters or leaves them into another part of the airgap. The elements making up the permeance are therefore defined as those having nodal potentials between the potentials of the nodes forming the corners of the tooth or slot element. The incremental permeances are then calculated by dividing the unslotted surface into a series of strips of width dx. The potential at each side of the strip is calculated by interpolating between the potential values at the nodes. The permeance of each strip is then calculated as described above. In this case, care must be taken to include elements which lie only partly within the strip. These are included by determining what proportion of the element is within the strip and including that proportion of the stored energy in the sum as shown in Figure 4. Figure 5 shows the possible cases of an element with respect to the flux lines. Having determined the variation of incremental permeance with angular position the harmonic permeances are calculated by the post-processor using a Fourier transform.

$$f_{r1} = \frac{A(m1) - A_0}{A(m1) - A(m2)}$$

$$f_{r2} = \frac{A(m1) - A_0}{A(m1) - A(m3)}$$

$$frac = f_{r1} * f_{r2}$$

$$e = B^2 * D * frac$$

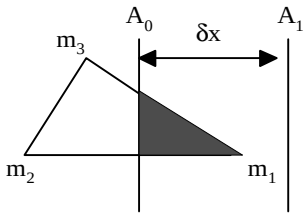

Fig. 4 Calculation of the stored energy of an element portion

4.1 Effect of slot current on normalised slot permeances

Since one of the aims of this project is to model the effect of closed rotor slots on the airgap field and on the permeance variation, it is clearly important to account for the rotor bar currents. The stator and rotor currents, hence the stator and rotor slot mmfs, increase as the load increases. The large rotor mmfs cause the slot

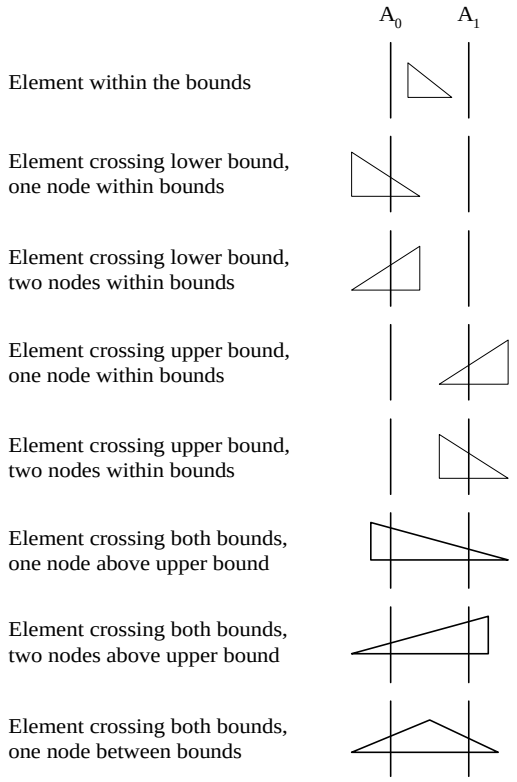

Fig. 5 The situations of an element w.r.t the flux lines

bridge or tooth tips in the semi-closed slots to saturate. The degree of saturation becomes larger for a closed slot machine and is a function of the rotor current. This saturation will cause the slots to appear as though they were semi-closed. This situation can be clearly seen in Figure 6 which shows the variation of normalised airgap permeance for different currents flowing through the bar. The mean permeance value decreases as the current amplitude rises due to the saturation effect while the permeance variations increase.

For a machine with closed slots, when the motor is loaded, the saturation of the slot bridge will cause the slots to have different spatial permeance functions according to the magnitude of the current enclosed in the slot. This varies approximately sinusoidally in space giving the permeance variation of Figure 7. The correct permeance harmonics can only be derived by evaluating them over one or two poles depending on the number of rotor slots. There is of course a low order sub harmonic of the slot permeance due to this saturation which rotates synchronously with the rotor current wave. The slot permeance harmonics themselves rotate with the angular velocity of the rotor.

It can be clearly seen in Figure 7 that closing the slots effectively removes the rotor slot permeance variations when there is no rotor current to saturate the slot bridge. The slots between 5 and 6 carry less current; therefore, the permeance variation across this slot is almost smooth.

Figure 8 shows the slot permeance variation of two semi closed slots with different slot openings. It is apparent that the larger the slot opening the higher the slot ripple, as expected.

A 56 semi-closed rotor slot has also been modelled by the same procedure. The resulting permeance variation for a half pole of the 4-pole machine is shown in Figure 9. The effect of tooth tip saturation is much less than for the slot bridge saturation of the closed slot rotor. The most significant feature is the absence of slots where there is virtually no permeance variation. However, for slots carrying the equivalent of full load current there appears to be not much difference between semi-closed and closed slot normalised permeance variations.

The amplitude of the slot permeance harmonics is obtained by applying a Fast Fourier Transform to the slot permeance distribution. The resulting normalised slotting permeance harmonic amplitudes are shown in Figure 10 and the coefficients of the first three harmonics of slot permeance as a percentage of the constant permeance for 56 closed slot is plotted in Figure 11 as a function of peak rotor slot current. Clearly, the higher the slot current the greater the content of higher harmonics.

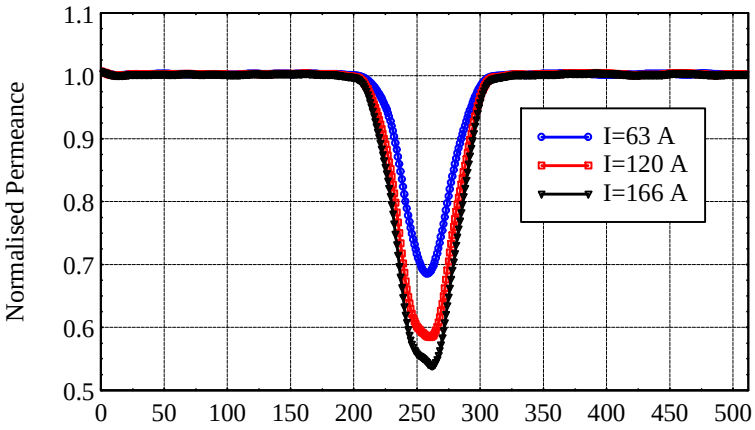

Fig. 6 Variation of permeance with different saturation conditions for 40 closed slot rotor (slot pitch divided into 512 strips)

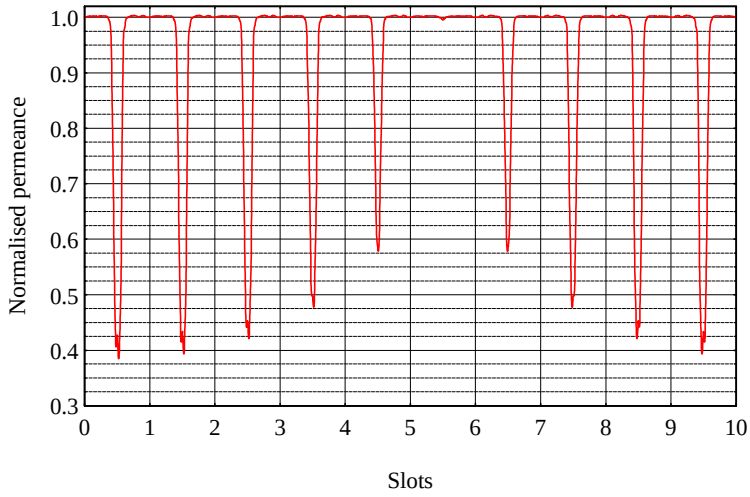

Fig. 7 The rotor slot permeance variation of a complete pole of a 40-closed-slot rotor under full load

Fig. 8 Permeance variation of a 56 slot rotor with different slot openings (Two slot pitches divided into 512 strips)

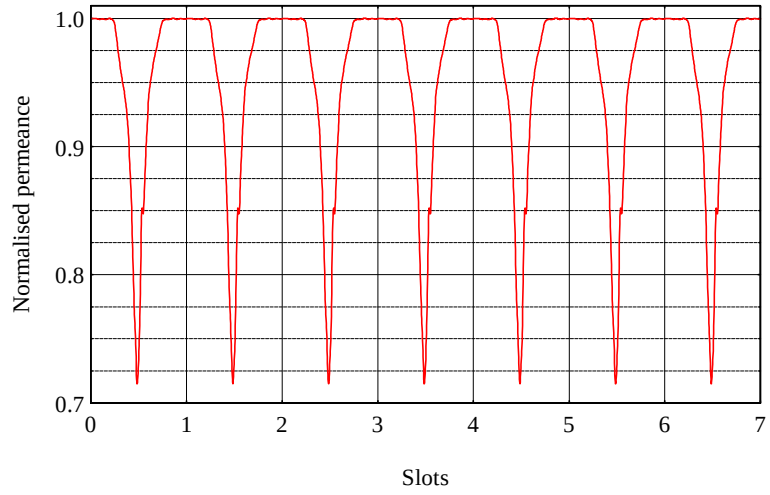

Fig. 9 The permeance variation of a half pole of a 56 semi-closed-slot rotor under full load

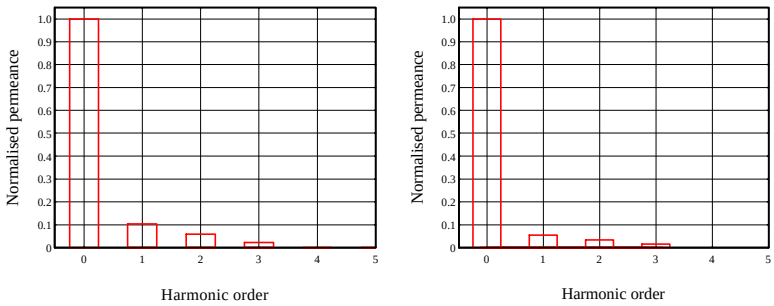

Fig. 10 Normalised permeance harmonics for a 56 closed slot rotor under full load and half load

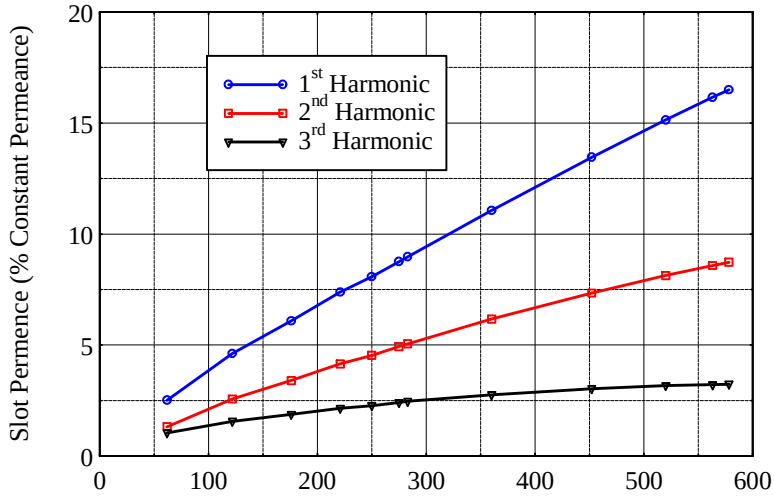

Fig. 11 Variation of slot permeance harmonic coefficients as a function of slot current of a 56 closed slot rotor obtained by FFT of slot permeance variations

5. CONCLUSION

The methods for evaluating the magnetic permeance harmonics introduced by saturation and slotting have been explained in this study. Distributed saturation effects of closed rotor slots due to differences between the bar currents at any time instant have been illustrated and their effects accounted for in the model.

In a given design of the induction machine the amplitude of the slot permeance wave is controlled mainly by whether the slots are open or closed. The open slot, especially with a small airgap, produces large permeance harmonics; however, the semi-closed slot produces harmonics of a small amplitude and it is attenuated by employing closed slots. The degree to which they are attenuated by changing from a semi-closed slot to an open slot is load dependent. At full load, because of the large rotor bar currents which cause the slot bridge to saturate, the airgap slot permeance ripple is larger than at half load and at no load.

6. REFERENCES

[1] A. Ferrah, K.J. Bradley and G.M. Asher, An fft based novel approach to non-invasive speed measurement in induction motor drives, *IEEE Instrumentation and Measurement*, Vol. 41, No. 6, pp. 797-802, 1992.

[2] S. Onodera and K. Yamasawa, Effect of stator slot opening on the electromagnetic vibration in a squirrel-cage induction motor, *Electrical Engineering in Japan*, Vol. 114, No. 2, pp. 133-146, 1994.

[3] J.H. Walker, A theory of induction motor surface losses, *IEE Proceedings*, Vol. 95, pt. II, pp. 597-603, 1948.

[4] J. Penman and M.N. Dey, Condition monitoring of electrical drives, *IEE Proceedings*, Vol. 133, pt. B, pp. 142-148, 1986.

[5] X. Deng and E. Ritchie, Detection of broken rotor bars in induction motor rotors, International Conference on Electrical Machines, pp. 164-169, 1993.

[6] E.M. Freeman, The calculation of harmonics, due to slotting, in the flux density waveform of a dynamo-electric machine, *IEE Proceedings*, Vol. 109, Pt. C, No. 16, pp. 581-588, 1962.

[7] H.M. Hesse, Air gap permeance in doubly-slotted asynchronous machines, *IEEE Transaction on Energy Conversion*, Vol. EC-7, No. 3, pp. 491-499, 1992.

[8] W.H. Press, B.P. Flannery, S.A. Teukolsky and W.T. Vetterling, *Numerical Recipes in Fortran: The Art of Scientific Computing*, Cambridge University Press, 1992.

[9] S. Williamson, L.H. Lim and M.J. Robinson, Finite element models for cage induction motor analysis, *IEEE Transactions on Industry Applications*, Vol. IA-26, No. 6, pp. 1007-1017, 1990.

[10] H. Guldemir, Prediction of induction motor line current spectra from motor design data, Ph.D. Thesis, University of Nottingham, 1999.

[11] I. Zagradi{nik and B. Hribernik, Influence of anisotropy of magnetic material on the saturation harmonics in the three phase induction motor, *IEEE Transactions on Magnetics*, Vol. MAG-24, No. 1, pp. 491-494, 1988.

[12] M.V.K. Chari and P. Silvester, Analysis of turbo alternator magnetic fields by finite elements, *IEEE Transactions on Power Apparatus and Systems*, Vol. PAS-90, No. 2, pp. 454-464, 1971.

[13] M.V.K. Chari and P. Silvester, Finite element analysis of magnetically saturated dc machines, *IEEE Transactions on Power Apparatus and Systems*, Vol. PAS-90, pp. 2362-2372, 1971.

[14] P.P. Silvester and M.V.K. Chari, Finite element solution of saturable magnetic field problems, *IEEE Transactions on Power Apparatus and Systems*, Vol. PAS-90, pp. 1642-1651, 1971.

[15] T. Nakata and K. Gakuin, Present situation and trends and what is needed for the future FEM analysis of electrical machines, Proc. of the Int. Conf. on Electrical Machines (ICEM'98), Istanbul, Turkey, Vol. 2, pp. 685-691, 1998.

[16] P.P. Silvester and R.L. Ferrari, *Finite Elements for Electrical Engineers*, Cambridge University Press, 1983.

ODRE \ IVANJE VARIJACIJE MAGNETSKE VODLJIVOSTI UTORA KOD INDUKCIJSKIH STROJEVA UZ UKLJU^IVANJE ZASI]ENJA MOSTA UTORA

SA@ETAK

U ovom radu koristi se metoda kona~nih elemenata za odre|ivanje varijacija magnetske vodljivosti utora oko zra~nog raspora kao i za odre|ivanje harmoni~nog sadr`aja kaveznog indukcijskog motora sa zatvorenim utorom. U radu se tako|er iznosi i sli~no rješenje, koje do sada nije bilo poznato, a odnosi se na varijacije magnetske vodljivosti utora, koje uzima u obzir zasi}enje jezgre do kojeg dolazi zbog nelinearnih karakteristika magnetskog materijala i zbog zasi}enja koje je posljedica induciranih struja šipke rotora koje su od velikog zna~aja.

Varijacija magnetske vodljivosti izvodi se iz uskladištene energije, a dobiva se kori{tenjem rješenja polja kona~nog elementa. Distribucija magnetske vodljivosti se zatim razla`e na harmoni~ni sadr`aj, koriste}i brzu Fourier-ovu transformaciju. Tako|er se prikazuje i ovisnost harmoni~nih elemenata o struji rotora.

***Klju~ne rije~i**: utor, zra~ni raspor, magnetska vodljivost, indukcijski motor, zasi}enje mosta utora.*